87-fs Pulse Generation in a Diode-Pumped SESAM Mode-Locked Yb:YLF Laser

FEDERICO PIRZIO[1,*], LUIGI FREGNANI[1], AZZURRA VOLPI[2], ALBERTO DI LIETO[2], MAURO TONELLI[2], AND ANTONIO AGNESI[1]

[1] Universita' di Pavia, Dip. di Ingengeria Industriale e dell'Informazione, Via Ferrata 5, 27100 Pavia, Italy
[2] NEST Istituto Nanoscienze-CNR and Dipartimento di Fisica, Universita' di Pisa, Largo B. Pontecorvo 3, IT-56127 Pisa, Italy
[*] Corresponding author: federico.pirzio@unipv.it

Compiled May 4, 2016

An Yb:YLF crystal has been investigated in a femtosecond oscillator pumped by two 400-mW single-mode fiber-coupled diodes emitting at 976 nm and mode-locked with a SESAM. Almost Fourier transform limited pulses with duration of 87 fs and 107 fs were demonstrated for extraordinary and ordinary polarization respectively. This is, to the best of our knowledge, the first demonstration of sub-100-fs pulses with Yb:YLF and it proves the potential for ultrashort pulse generation and amplification with this material.

OCIS codes: *(140.7090) Ultrafast lasers; (140.3380) Laser materials; (140.3615) Lasers, ytterbium.*

http://dx.doi.org/10.1364/ao.XX.XXXXXX

1. INTRODUCTION

Several host materials (e.g. tungstates [1, 2] , oxides [3, 4], fluorides [5, 6]) have been proposed for Yb doping in view of ultrafast pulse generation and amplification, each of them with peculiar and complementary characteristics. Among these different hosts, fluoride crystals are interesting because of their excellent thermo-optical properties, lower refractive index which limits unwanted nonlinear effects under intense laser pumping, low phonon energy reducing radiative relaxation between adjacent energy levels and a significant energy storage capability, particularly attractive for high energy pulse amplification [6]. So far, the shortest pulses obtained with a Yb-fluoride materials are 48 fs in a Yb:CaF_2 Kerr lens mode-locked (KLM) laser [7]. Despite this outstanding result, exploiting the more reliable SESAM mode-locking (ML) technology, 65-fs pulses have been demonstrated with this material only recently [8]. The main challenge with this material is its small value of emission cross section σ_e yielding high-energy storage capability. This can be responsible of SESAM optical damage in the presence of Q-switched mode-locking (QML) instabilities [9]. Compared to CaF_2, YLF host has interesting properties. In particular it offers a higher peak value of σ_e, similar thermal conductivity and thermo-optic coefficients, and it is naturally birefringent, hence it does not suffer of depolarization effects even in presence of significant thermal load [10].

In this work we present what is to the best of our knowledge, the first sub-100-fs Yb:YLF ML oscillator. Exploiting single-mode diode pumping and SESAM soliton ML, we were able to obtain 87-fs, (almost) Fourier transform limited pulses at 1052 nm, for the crystal orientation with emission parallel to the *c*-axis. Slightly longer (107 fs duration) pulses were obtained for the emission perpendicular to the *c*-axis.

2. EXPERIMENTS

The experimental setup for continuous wave (cw) and ML experiments is shown in Figure 1.

The active medium was a 10%-doped, 2.1-mm long, uncoated Yb:YLF sample, grown by the Czochralski method [11]. The growth process was carried out in a Czochralski furnace, dedicated to the growth of high-purity fluorides, equipped with resistive heating and optical automated diameter control. High-purity raw materials of LiF, YF_3 and YbF_3 compounds with guaranteed 5N purity (99.999%) were used as starting materials. LiF and YF_3 compounds were mixed in the relative concentrations 52.5% (LiF): 47.5% (YF_3), in accordance to the incongruent melting point of the YLF crystal. A proper amount of YbF_3 was added to the LiF-YF_3 mixture to obtain a 10at.% Yb doping level. Prior to melting, the growth chamber was evacuated down to 10^{-5} Pa in order to remove moisture and water vapor molecules, strongly reactive with fluorine at high temperatures with consequent formation of detrimental OH^- radicals in the melt. Melting and growth were then carried out under high-purity (5N) Ar and CF_4 atmosphere. The CF_4 enriched atmosphere is required for preventing inclusion of Yb^{2+} impurities, which form after reduction of Yb^{3+} ions in the melt. Such impurities, as OH^- radicals, if incorporated in-

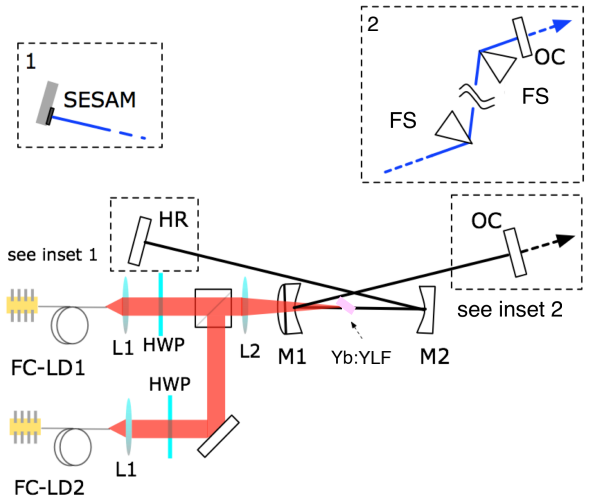

Fig. 1. Experimental setup for cw and ML experiments. FC-LD: Single-mode fiber-coupled laser diode; L1: Aspherical lens (f=15.3 mm, NA 0.16); HWP: Half-wave plate anti-reflection (AR) coated at 976 nm; L2: Spherical lens (50 mm focal length); M1: Concave mirror, R=50 mm, high reflectivity (HR) at 1000-1100 nm, high transmissivity at 940-980 nm; M2: Concave mirror, 100 mm radius of curvature; HR: Flat mirror HR between 1000-1100 nm; OC: Output coupler, 30' wedge; FS: Fused silica dispersive prisms; SESAM: Semiconductor saturable absorber mirror.

side growing crystals strongly degrade the optical quality of finished samples. A YLF undoped seed, oriented along the a-axis, was used to induce the oriented crystallization of the molten materials. During the growth, the pulling rate was 0.5 mm/h and the rotation rate 5 RPM (rounds per minutes). The growth temperature varied between 863 and 867 °C. After the growth, the absence of internal defects, such as cracks or microbubbles, was checked observing the propagation of non-absorbed laser beams through the volume of the sample. X-ray backscattering diffraction by means of Laue technique was used to determine the orientation of the optical axes and for checking the absence of polycrystalline nuclei. For these measurements, the sample was fixed inside a Laue chamber and irradiated by X-ray beam. Simulations of back-scattering diffraction patterns confirmed homogeneous growth along the *a*-axis of the unit cell and allowed to determine the orientation of the optical axes with uncertainty below 2°. Diffraction patterns acquired from different areas showed a single spot structure, without double or deformed marks which would indicate a polycrystalline structures related to staggered lattices formed during the growth.The absence of major contaminants was checked acquiring the absorption spectrum of the sample between 200 nm and 2.5 μm.

In the laser experiments, the pump module consisted of a couple of single-mode fiber-coupled laser diodes, each emitting a maximum power of 400 mW at 976 nm. By optimizing coiling the single-mode fiber pigtails we were able to induce a strongly elliptical polarization in each laser diode, with a ratio of about 13:1 between the two axes. The two beams were then combined and spatially overlapped in a polarizing beamsplitter cube, and eventually focused in the active medium to a beam radius $w_p \approx 12$ μm by means of the spherical lens L2.

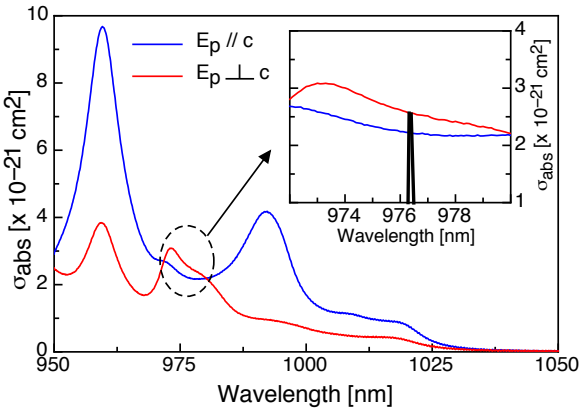

Fig. 2. Yb:YLF Absorption cross section for both polarizations of the pump beam. In the inset we show in more detail the spectral region around 976 nm and the pump laser diode spectrum.

In order to minimize insertion losses, we oriented the crystal at Brewster angle. This forced the oscillator to emit with field polarization E_L in the plane of Fig. 1. Given the YLF ordinary and extraordinary refractive indexes ($n_e \simeq 1.47$, $n_o \simeq 1.45$), we estimate a Fresnel reflection loss of about 12.5% for the half of the total incident pump which was perpendicularly polarized with respect to the incidence plane at the Brewster interface. Considering this reflection loss and the transmission of all the optical components of the pump module, the maximum incident pump power at 976 nm in our experiments was about 600 mW. As a consequence of Yb:YLF birefringency in combination with Brewster-angle crystal placement, the pump beam experiences walk-off in the tangential plane for the two different pump polarizations. Given the relatively small difference between ordinary and extraordinary refractive indexes, this traduces in a lateral displacement of the pump beam centroid for the two polarizations of only about 12 μm/mm inside the crystal. In our experimental setup in which we exploited the excellent pump beam quality to design a resonator with a very small cavity mode radius inside the active medium, this effect could not be neglected and contributed, together with pump beam confocal parameter considerations, to the identification of the optimal crystal length.

In Figure 2 we report the absorption spectrum of Yb:YLF for both polarizations (parallel and perpendicular to *c*-axis). The main absorption cross section peak of both polarizations occurs near 960 nm, but it is markedly different. Moreover, at this peculiar wavelength, high-power pump laser diodes are not widely available on the market. Conversely, close to 976-nm pump wavelength, as it is shown in the inset of Figure 2, the absorption cross section profile is smooth and the absolute value of cross section is similar for both polarizations and still high enough to permit reasonable pump absorption in few mm long crystals. This is clearly beneficial also in view of potential pump power up scaling with multi-mode, circularly polarized, multi-Watt fiber coupled laser diodes. In our experiments about half of the incident pump power was absorbed under lasing conditions for both crystal orientations.

The laser cavity was a standard X-folded design, optimized for cavity mode astigmatism compensation through a proper choice of the folding angles of curved mirrors M1 and M2. In

both cw and ML operation, the resonator was designed to operate in the stability region corresponding to larger separation M1-M2. Therefore, we could fine-tune the cavity mode waist on the HR/SESAM mirror by properly adjusting its distance to M2 and the M1-M2 separation. In cw and ML regime, the cavity arm lengths were as follows: M2-M3 = 260 mm; M1-M2 = 88 mm; M1-OC = 1150 mm. Through ABCD modeling we could estimate a fundamental cavity mode radius in the active medium $w_x \times w_y = 16 \times 11$ μm within the stability region, reasonably well matched to the pump radius. The results obtained in CW regime for a set of different output couplers (OCs) and for both the Yb:YLF sample orientations are shown in Figure 3.

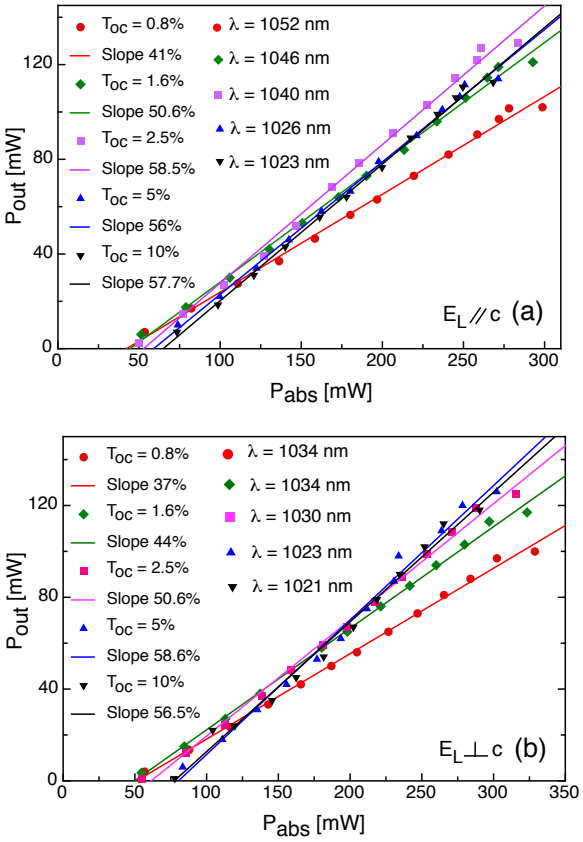

Fig. 3. CW measurements results. (a) Crystal oriented for emission parallel to *c*-axis; (b) Crystal oriented for emission perpendicular to *c*-axis.

The overall performance of the laser in cw regime was similar for both crystal orientations. A maximum output power of 129 mW was obtained with T = 2.5% OC for crystal orientation corresponding to $E_L \parallel c$ (absorbed pump power was 284 mW in this case). The maximum power obtained with $E_L \perp c$ was 126 mW with a T = 5% OC (corresponding absorbed pump power was 300 mW). A maximum slope efficiency close to 60% was measured for both the possible crystal orientations. This result represents an improvement of a factor ~ 2 with respect to previously reported results [12] and it is an indirect confirmation of the optimum resonator design and sample quality. The central output wavelengths measured for the different OC transmission for both polarization are in fairly good agreement with what could be expected by the emission cross section and spectral gain curves reported in ref. [13]. We also carried out a Caird

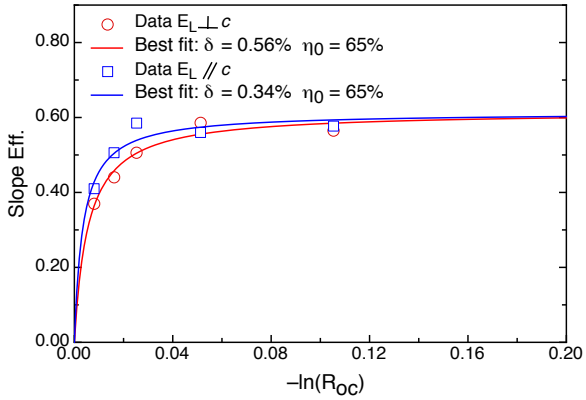

Fig. 4. Caird slope analysis results. The blue dots and line refer to the crystal oriented for emission parallel to *c*-axis; the red dots and line refer to the crystal oriented for emission perpendicular to *c*-axis.

slope analysis [14] in order to asses the resonator losses δ (not comprising reabsorption losses) and sample intrinsic slope efficiency η_0 for both crystal orientations. The results are shown in Figure 4. The slightly lower value of δ in case of emission parallel to crystal *c*-axis is likely due to a better Brewster angle orientation.

For ML experiments we replaced the HR mirror in Fig. 1 with a SESAM (3% modulation depth, 140 μJ/cm^2 saturation fluence, Spectra Physics Rankweil). Group Delay Dispersion (GDD) compensation was realized with a pair of fused silica dispersive prisms. The optimum prisms separation was 60 cm tip-to-tip, corresponding to a maximum negative GDD of about -1300 fs^2. The optimization of the resonator in soliton ML regime was achieved following the design concepts outlined in ref. [8]. For materials exhibiting long fluorescence lifetime and relatively small value of the peak emission cross section, a careful selection of the cavity mode dimension over the SESAM is crucial to prevent optical damages of the SESAM in presence of QML instabilities in the early stage of resonator optimization. In our experiments ML was self-starting once all the cavity parameters (alignment, prisms insertion, M1-M2 distance) were optimized. Best results in term of both shortest pulse duration and long term stability were obtained for a total cavity length of 1.50 m, corresponding to a ML pulse repetition rate of 100 MHz. In these conditions a minimum pulse duration of 87 fs with 35-mW average output power was obtained for the extraordinary laser polarization employing a T = 0.8% OC.

The corresponding optical spectrum was 14 nm full width at half maximum (FWHM) wide and centered at 1052 nm (see Fig. 5(a)), yielding a time-bandwidth product ≈ 0.33, very close to Fourier transform limit for sech^2 shaped soliton ML pulses. A minimum pulse duration of 107 fs with 29-mW average output power was obtained for the ordinary laser polarization with the same OC. The corresponding optical spectrum was 11.2 nm FWHM wide and centered at 1043 nm (see Fig. 5(b)), still yielding a nearly transform-limited product ≈ 0.33. This represents a reduction of a factor >2 of the pulse duration with respect to previously reported results for Yb:YLF [13]. Wider spectra and shorter pulses were always obtained working at the maximum available pump power. A reduction of the pump power systematically resulted in narrower spectra and longer pulse duration. This behavior suggests that our results were limited by the

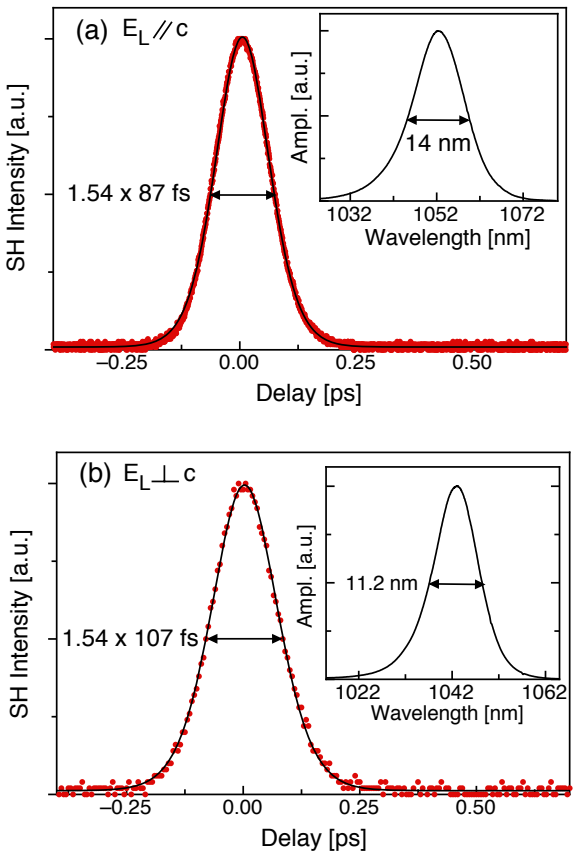

Fig. 5. Autocorrelation trace and optical spectrum of the shortest pulse obtained for (a) parallel to *c*-axis emission and (b) perpendicular to *c*-axis emission.

available pump power (hence intracavity pulse energy) rather than by the available gain bandwidth of the material. ion in cw regime, with best slope efficiency close to 60%, and 87-fs long ML pulse trains with 35 mW average output power for the laser emission with polarization parallel to *c*-axis. This result shows the potential of Yb:YLF for generation or amplification of ultrashort pulses. The good material quality and its thermal features, as well as nearly polarization-independent absorption at the very convenient 976-nm pump wavelength, look promising for power scaling.

3. CONCLUSIONS

We have reported what is, to the best of our knowledge, the first demonstration of mode-locking in a diode-pumped Yb:YLF laser with pulses shorter than 100 fs. This result was obtained pumping with two polarization-combined 400-mW, fiber coupled single-mode laser diodes emitting at 976 nm. Despite pumping with significant detuning from the peak absorption cross section wavelength, we were able to demonstrate efficient laser operation in cw regime, with best slope efficiency close to 60%, and 87-fs long ML pulse trains with 35 mW average output power for the laser emission with polarization parallel to *c*-axis. This result shows the potential of Yb:YLF for generation or amplification of ultrashort pulses. The good material quality and its thermal features, as well as nearly polarization-independent absorption at the very convenient 976-nm pump wavelength, look promising for power scaling.

4. FUNDING INFORMATION

A.Volpi acknowledges support by the European Space Agency under grant No. 4000108074/13/NL/PA – "Cooling Effect on Fluoride Crystals".

REFERENCES

1. N. V. Kuleshov, A. A. Lagatsky, A. V. Podlipensky, V. P. Mikhailov, and G. Huber, "Pulsed laser operation of Yb-doped $KY(WO_4)_2$ and $KGd(WO_4)_2$," Opt. Lett. **22**, 1317–1319 (1997).
2. F. Brunner, G. J. Spühler, J. Aus der Au, L. Krainer, F. Morier-Genoud, R. Paschotta, N. Lichtenstein, S. Weiss, C. Harder, A. A. Lagatsky, A. Abdolvand, N. V. Kuleshov, and U.Keller, "Diode-pumped femtosecond Yb:$KGd(WO_4)_2$ laser with 1.1-W average power," Opt. Lett. **25**, 1119–1121 (2000).
3. A. Yoshida, A. Schmidt, V. Petrov, C. Fiebig, G. Erbert, J. Liu, H. Zhang, J. Wang, and U. Griebner, "Diode pumped mode-locked Yb:YCOB laser generating 35 fs pulses," Opt. Lett. **36**, 4425–4427 (2011).
4. E. Caracciolo, M. Kemnitzer, A. Guandalini, F. Pirzio, J. Aus der Au, and A. Agnesi, "28-W, 217 fs solid-state Yb:$CAlGdO_4$ regenerative amplifiers," Opt. Lett. **38**, 4131–4133 (2013).
5. S. Ricaud, F. Druon, D. N. Papadopoulos, P. Camy, J.-L. Doualan, R. Moncorgé, M. Delaigue, Y. Zaouter, A. Courjaud, P. Georges, and E. Mottay, "Short-pulse and high-repetition-rate diode-pumped Yb:CaF_2 regenerative amplifier," Opt. Lett. **35**, 2415–2417 (2010).
6. F. Druon, S. Ricaud, D. N. Papadopoulos, A. Pellegrina, P. Camy, J. L. Doualan, R. Moncorgé, A. Courjaud, E. Mottay, and P. Georges, "On Yb:CaF_2 and Yb:SrF_2: review of spectroscopic and thermal properties and their impact on femtosecond and high power laser performance," Opt. Mater. Express **1**, 489–502 (2011).
7. P. Sévillano, G. Machinet, R. Dubrasquet, P. Camy, J.-L. Doualan, R. Moncorgé, P. Georges, F. Druon, D. Descamps, and E. Cormier, "Sub-50 fs, Kerr-lens mode-locked Yb:CaF_2 laser oscillator delivering up to 2.7 W," in Advanced Solid-State Lasers Congress, OSA Technical Digest (Optical Society of America, 2013), paper AF3A.6.
8. F. Pirzio, S. D. Di Dio Cafiso, M. Kemnitzer, F. Kienle, A. Guandalini, J. Aus der Au, and A. Agnesi, "65-fs Yb:CaF_2 laser mode-locked by semiconductor saturable absorber mirror," J. Opt. Soc. Am. B **32**, 2321–2325 (2015).
9. C. Honninger, R. Paschotta, F. Morier-Genoud, M. Moser, and U. Keller, "Q-switching stability limits of continuous-wave passive mode locking," J. Opt. Soc. Am. B **16**, 45–56 (1999).
10. P. Aballea, A. Suganuma, F. Druon, J. Hostalrich, P. Georges, P. Gredin, and M. Mortier, "Laser performance of diode-pumped Yb:CaF_2 optical ceramics synthesized using an energy-efficient process,"Optica **2**, 288–291 (2015).
11. B. Pamplin, "Crystal growth," Pergamon Press, Oxford, U.K., (1975).
12. N. Coluccelli, G. Galzerano, L. Bonelli, A. Toncelli, A. Di Lieto, M. Tonelli, and P. Laporta, "Room-temperature diode-pumped Yb^{3+}-doped $LiYF_4$ and KYF_4 lasers," Appl. Phys. B **92**, 519–523 (2008).
13. N. Coluccelli, G. Galzerano, L. Bonelli, A. Di Lieto, M. Tonelli, and P. Laporta, "Diode-pumped passively mode-locked Yb:YLF laser," Opt. Express **16**, 2922–2927 (2008).
14. J. A. Caird, S. A. Payne, P. R. Staber, A. J. Ramponi, L. L. Chase, and W. F. Krupke, "Quantum electronic properties of the $Na_3Ga_2Li_3F_{12}$:Cr^{3+} laser," IEEE J. Quantum El. **24**, 1077–1099 (1988).